Service Robots Assisting Human: Designing, Prototyping and Experimental Validation

Y. Maddahi, S. M. Hosseini Monsef, A. Maddahi and R. Kalvandi

Abstract— This paper addresses the design, prototyping and experimental validation of two different types of wheeled mobile machine, employed as service robots to assist the human. The focus is on the explanation of modeling and design procedure as well as the optimization of robot positioning during the motion along some given and unseen trajectories. Using the coordination defined for mobile robots, the equations of motion are firstly derived and then the simulation study is carried out. Using the simulation results, the robots are prototyped. Next, to overcome the positioning errors, the mobile robots are tested and moved along some given paths. The position error consists of systematic and non-systematic errors. As pointed out, the systematic errors are modified and reduced using benchmark method where the absolute measurements of errors are compared with the desired posture of robots. Specifically, the results derived from experimental analyses concede that in the mean error improvement was at least 83% in both CW and CCW directions. The procedure explained in this paper should therefore be considered seriously as a new tool to design the wheeled mobile robots.

Keywords— Design process, Service robot, Differential drive mechanism, Experimental validation.

I. Introduction

WHEELED mobile robots (WMRs) are extensively used in robotics, since their motion is easy to program and can be well controlled. Differential drive WMR is a mobile robot whose movement is based on two separately driven wheels placed on either side of the robot body. Using differential drive mechanism, the robot is capable of changing its direction by varying the relative angular velocity of wheels and hence does not require an additional steering motion. During the robot motion depending on the robot body orientation, the centre of rotation may fall anywhere in the line joining the wheels together (wheelbase) which usually creates some positioning errors. By using proper calibration, the accuracy of robot during motion can be increased.

There exist several factors such as design purposes and surrounding parameters which affect the design of the mobile robot directly. By using these factors, the design procedure and manufacturing system can be broken into sub-systems including design philosophy, technical definitions, modeling and simulation method, quality control and risk assessment approaches, available manufacturing technologies and test/calibration method. To maintain the consistency of the whole system, an interface layer is usually proposed to facilitate the communication between these subsystems and set the protocols that enable the interaction between the subsystems to take place. In spite of the fact that the engineers and researchers usually do their best to implement the best devices and machines to fabricate a robot, existence of some imperfections during the design, manufacturing and assembly processes are unavoidable. This usually creates some positioning errors which by using proper calibration, the accuracy of robot during motion can be increased. Calibration is defined as a set of operations that establishes, under specified conditions, the relationship between the values of quantities indicated by a measuring instrument and the corresponding values realized by standards [1]. There are several methods used for calibration of robotic systems. They include odometry [2], 3D camera error detecting [3], active beacons [4], gyroscope [5] and magnetic compasses [6].

For mobile robots, the organized test procedure remains to be one of the most important means of achieving position error reduction. For instance, benchmark series are the use of data from the movement of actuators to estimate change in position over time [7-12]. They are widely used by various types of mobile robots, whether they be legged or wheeled to estimate (not determine) their position relative to a starting location. On the other hand, the purpose of the experimental tests which are dependant to time is to build an incremental model of the motion using measurements of the elementary wheel rotations. This type of experiment can be applied to measure and then reduce the errors of mobile robots which can be categorized into vehicles equipped with wheels such as general robots (automobile-type) and two degrees of freedom robots with two parallel wheels (two-wheeled) or some caster wheels (differential drive).

This paper focuses on design, modeling and calibration of two different types of differential drive mobile robots used as vacuum cleaner machine and searching robot which were motivated by a necessity for researching goals to fabricate cost-effective robot capable of cleaning the constructed environments and searching through the unconstructed environment. Section 2 addresses the measurement system and control algorithm of differential drive mobile robots followed by the characteristics of prototype robots. Section 3 addresses the kinematics and dynamic equations of the differential drive mobile robots. Then, in order to validate the derived equations, the consequences of simulation are carried out in Adams software. The results of modeling and simulation are covered in Section 3. Section 4 discusses on the odometry approach used to measure the robot systematic errors. The conclusions are presented in Section 5.

Y. Maddahi is with the Mechanical and Manufacturing Engineering Department, University of Manitoba, Winnipeg, MB, Canada (e-mail: y_maddahi@umanitoba.ca).

S. M. Hosseini Monsef is with the Department of Mechanical Engineering at Saveh Branch, Islamic Azad University, Saveh, Iran (e-mail: seyyed.mhm@gmail.com).

A. Maddahi is with the Mechanical Engineering Department at the K. N. Toosi University of Technology, Vanak Sq., Tehran, Iran (e-mail: amaddahi@sina.knt.ac.ir).

R. Kalvandi is with the Department of Science, University of Winnipeg, Winnipeg, MB, Canada (kalvandi-r@iam.uwinnipeg.ca).

II. Design and Control System

A. Measurement System and Camera Positioning

In this study, the camera positioning technique is used to obtain the coordinates (position and orientation) of robot during the motion in two-dimensional space. To transform the coordinates of cameras to global reference coordinate $\{X_R Y_R\}$, the scaling technique is used which maps the position recorded by center of mass in the taken photo to the global position of this point. With images taken by these two fixed cameras, the position of robot is calculated and its coordinates in horizontal plane are obtained. As shown in Fig. 1, for this robot, two stationary cameras are looking at the robot. One of these cameras is fixed and zooms along X_G-axis (camera 1) and the second one is located in Y_G-axis direction (camera 2). Position of robot is determined in image plane and then transferred to global coordinate by using derived transformation matrices (see Section III) and Denavit-Hartenberg notations [13]. Indeed, the cameras take the sequences of photo from the robot (record the position of $\{X_b Y_b\}$ frame) and the encoders count pulses of motors and finally, the taken pictures are scaled and the robot, as a target, is recognized among other objects. Next, based on the input desired path and considering the counted pulses which are read from incremental encoders, the amount of errors is calculated. Figure 1 depicts the top view of coordination system considered for experiments as well as the control algorithm of position determination of mobile robot during the tests.

B. Control System of Robots

The control block diagram of robots is shown in Fig. 2. The external sensors directly affect the robot decision algorithm. Moreover, it denotes that the collection of forward block diagrams can minimize the robot errors in motion using external sensors. The "Jacobian Matrix" block, changes the angular displacement or velocity obtained from "Robot" block to linear displacement or velocity in order to compare them with the path parameters and calculate the error function.

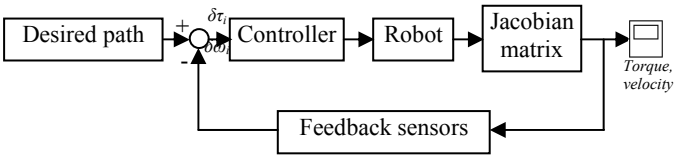

Fig. 2. Control block diagram of robots.

Figure 3 illustrates the decision algorithm of both mobile robots. As shown in this figure, controller can calibrate the robot errors during the robot movement. In Fig. 3, θ_{max}, ω_{max} and τ_{max} are the maximum allowable angular displacement, angular velocity and torque of actuators which are determined by user according to the motors used in the robot structure.

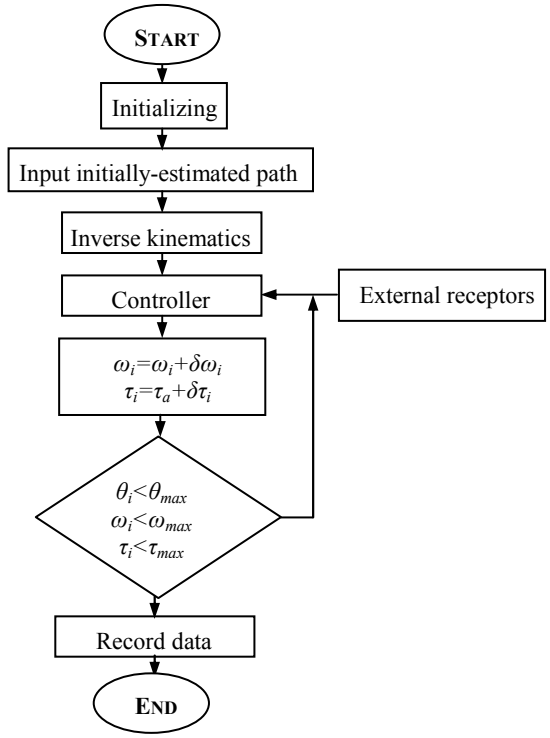

Fig. 3. Decision flow chart of robots. $\delta\omega_i$ and $\delta\tau_i$ represent the error functions of motors angular velocities and torques (Fig. 2).

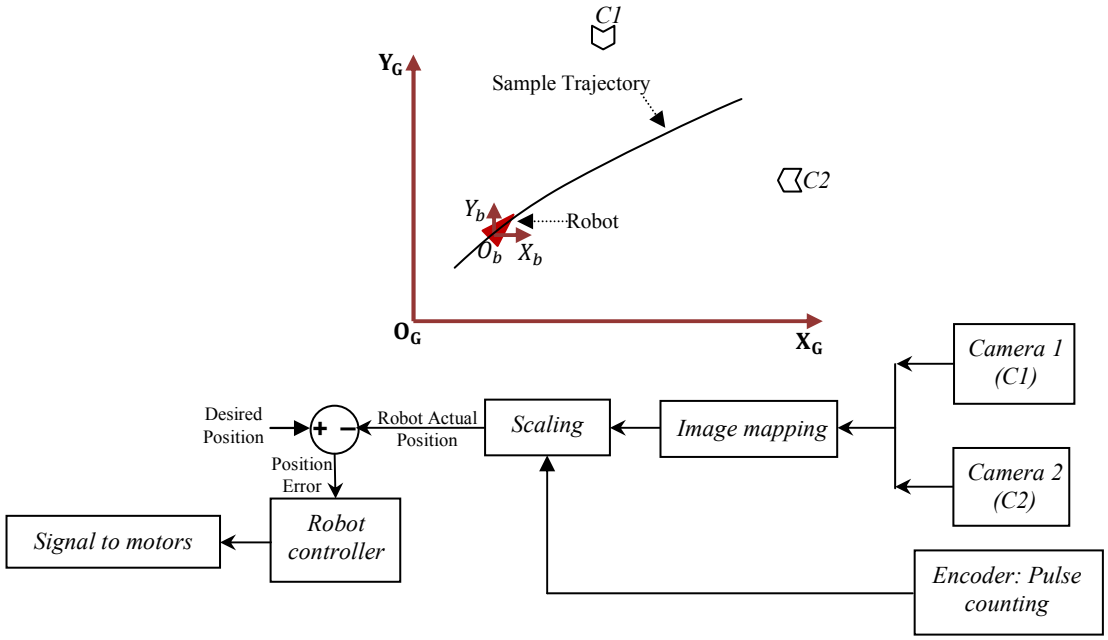

Fig. 1. Position-based control system used for both robots. Test plate is a 5×5 m^2 square.

C. Robots Structure

The construction of the cleaner robot (R1) consisting of two driving wheels with associated gear box, two shafts that connect the wheels to gearbox, three sensors to detect the collision and vacuum board is depicted in Fig. 4. The vacuum cleaner robot works in two self-controlled and remote control modes. This robot is designed for navigation with high maneuverability on flat and low friction surfaces [14].

The structure of searching robot, R2, is shown in Fig. 5. The construction of the robot comprises of two driving wheels, two spur gear boxes, a system for visually data recording, two ultrasound sensors for obstacle detection, electrical system and the jumping mechanism. The jumping mechanism includes two small DC motors for locking the wheels, a DC motor, collection of mechanical springs, a spur gear box and corresponding pulley system [15].

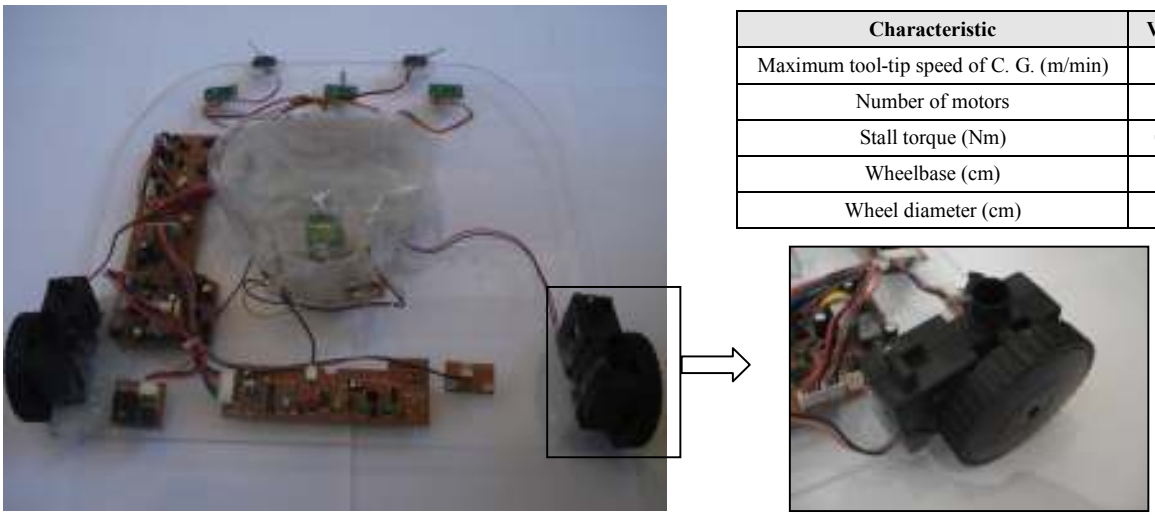

Characteristic	Value
Maximum tool-tip speed of C. G. (m/min)	3.5
Number of motors	3
Stall torque (Nm)	0.28
Wheelbase (cm)	135
Wheel diameter (cm)	35

Fig. 4. Structure of vacuum cleaner robot.

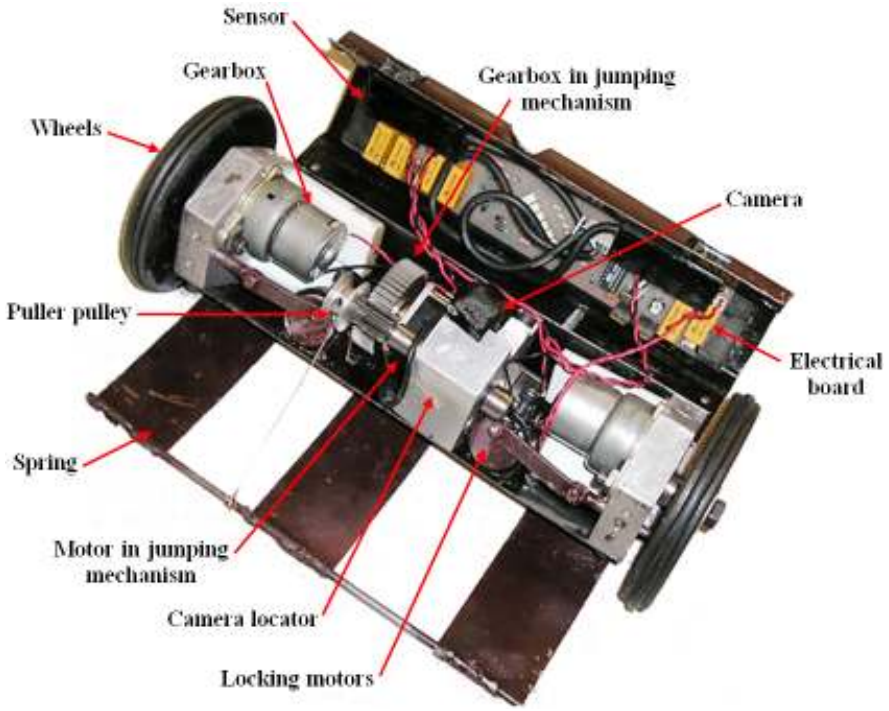

Characteristic	Value
Maximum tool-tip speed of C. G. (m/min)	1.15
Number of motors	5
Stall torque (Nm)	0.2
Wheelbase (cm)	115
Wheel diameter (cm)	50

Fig. 5. Structure of searching robot.

III. Mathematical Modeling of Mobile Robot

The general diagram of a planar differential drive mobile robot is shown in Fig. 6. Each wheel is assumed to rotate independently and without slippage. The kinematics equations of this robot are obtained using Denavit-Hartenberg notation [13]. Based on these equations, independent non-holonomic constraints due to instant no-slip wheel conditions are written as follows:

$$\dot{x}\,cos(\theta) + \dot{y}\,sin(\theta) - 0.5\left(r_R\dot{\theta}_R + r_L\dot{\theta}_L\right) = 0 \quad (1)$$

$$\theta = \left(\frac{1}{l}\right)(r_R\theta_R - r_L\theta_L) \quad (2)$$

$$\dot{x}\,sin(\theta) = \dot{y}\,cos(\theta) \quad (3)$$

where l indicates the wheelbase, x and y are the generalized coordinates of the frame with respect to the reference coordinate $\{X_R Y_R\}$, θ represents the orientation of the robot with respect to the initial position of robot at the start of motion and r is the radius of wheels. The parameters are illustrated in Fig. 6.

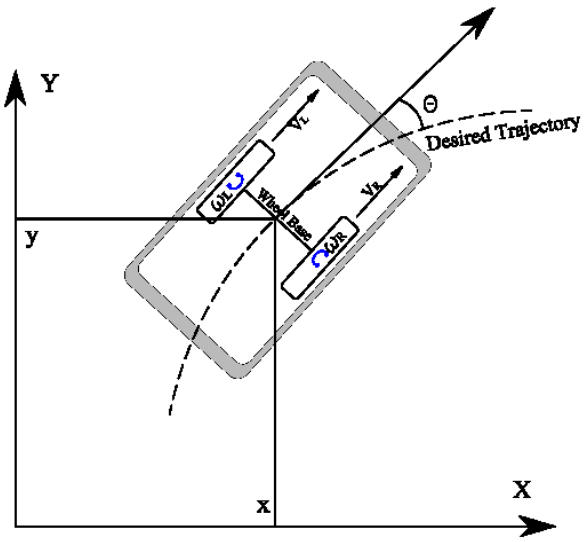

Fig. 6. Coordinate system of mobile robot.

Using the Lagrangian technique, the dynamic formulations of robot are expressed by the following equations [15]:

$$M[\ddot{x}\,cos(\theta) + \ddot{y}\,sin(\theta)] + 0.5mr\left(\ddot{\theta}_R + \ddot{\theta}_L\right) = (\tau_R + \tau_L)/r \quad (4)$$

$$l\ddot{\theta} = 0.5mrl\left(\ddot{\theta}_L - \ddot{\theta}_R\right) + l(\tau_L - \tau_R)/r \quad (5)$$

where M and m are the masses of the robot and each wheel, respectively and r is the radius of wheels. τ_L and τ_R denote the input torques of left and right actuators, $(\dot{\theta}_R, \dot{\theta}_L)$ and $(\ddot{\theta}_R, \ddot{\theta}_L)$ denote the angular velocities and accelerations of robot motors.

In order to validate the kinematics and dynamics equations, a model of cleaner robot was analyzed using the student version of Adams software. The robot is programmed to move along different trajectories and the results were compared with the theoretical values. In this study, the small-detailed components such as electrical wires were ignored. Figure 7-a shows a typical trajectory obtained using simulation study. It can be seen that there exist some differences between the desired and actual paths. The errors are originated from this fact that in theoretical modeling, some effective parameters such as misalignment in joints and friction force are usually neglected. Furthermore, Fig. 7-b illustrates the torques of left motor for this robot in the trajectory considered in Fig. 7-a. As illustrated, in simulation study, the robot needs extra torque to move along given path compared to the theoretical value of torque. For instance, as shown in Fig. 7-b, the torque of left motor has the maximum value of 52 Nmm while the minimum torque is about 40 Nmm.

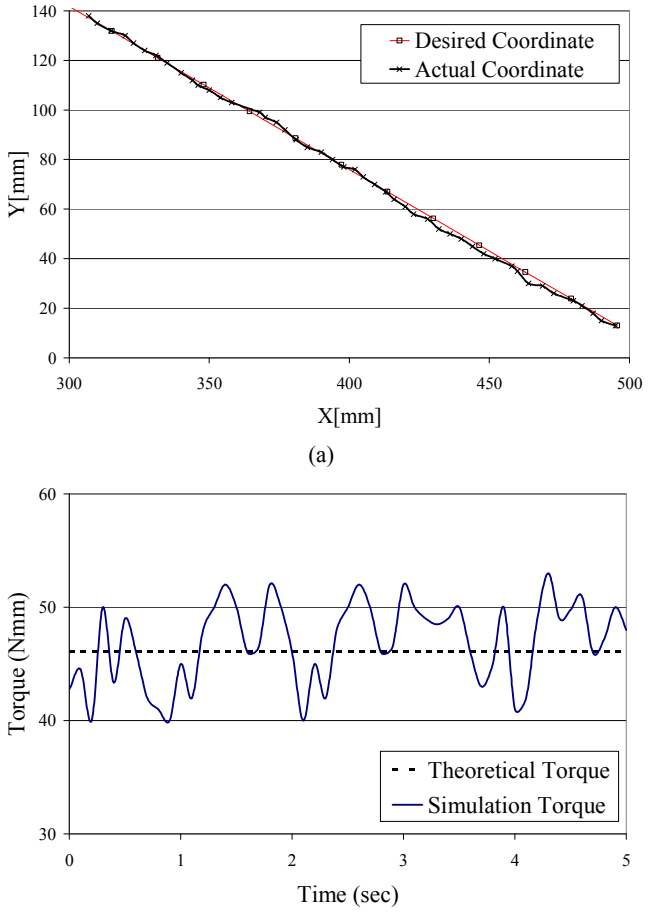

Fig. 7. Typical desired and actual trajectories and torques derived for left actuator of vacuum cleaner robot.

Figure 8-a illustrates a typical trajectory of robot which the model is programmed to move at the constant speed of 0.25 m/s along a straight line. Figure 8-b depicts the torques of left and right motors along the same trajectory. As shown, the torque of left motor possesses the maximum value of 140.6 Nmm while the minimum torque is about 134.6 Nmm. The error values of actuators torque are calculated using $\bar{\tau}_e = \bar{\tau}_{act.} - \bar{\tau}_{des.}$. Indeed, $\bar{\tau}_e$ is the difference between the mean

value of actual torque, $\bar{\tau}_{act.}$, obtained from the software output and the mean value of desired torque ($\bar{\tau}_{des.}$) obtained from analytical solution. Implementing this approach in simulating the robot helps us have the more accurate estimation of position, velocity, torque and force as opposed to analytical solution. Using data shown in Fig. 8-b, two motors with torque of 200 Nmm, which is obtained by the factor of safety equal to 1.36, were chosen for R2. The factor of safety is determined by the designers according to motor specifications and the level of risk in the system.

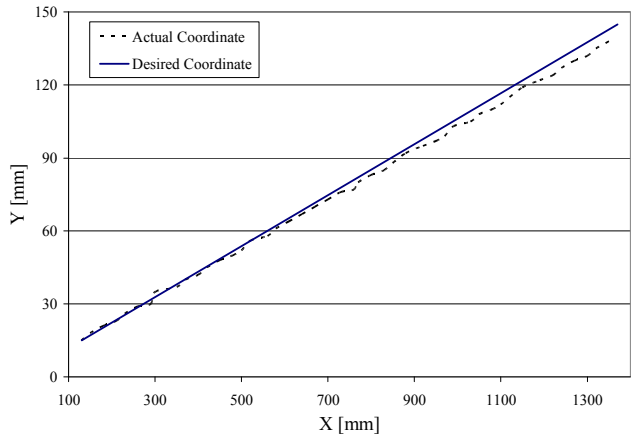

(a)

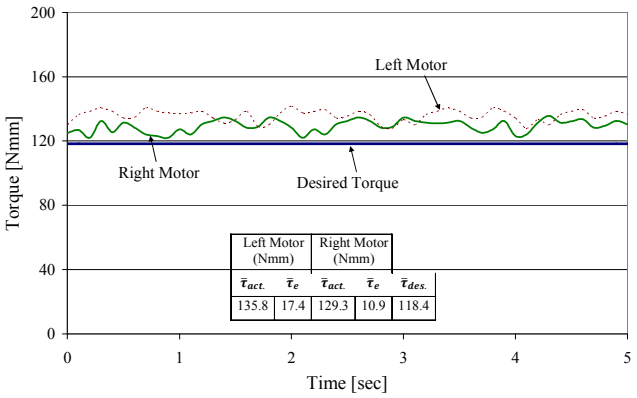

(b)

Fig. 8. Typical desired and actual trajectories and torques derived for right actuator, R2.

IV. Experimetal Results

One of the methods for measuring odometry errors is benchmark series test which allows the experimenter to draw conclusions about the overall odometric accuracy of the robot. The first benchmark method applied on robot for error correction is called “UMB mark” with sub-test named "Uni-Directional square path (UDT) Test. The robot starts out at a position which is labeled "Start" and move on a 4×4m uni-directional square path. The robot is programmed to travel the four legs of the square path but because of odometry and controller errors, not precisely to the starting position [7].

Another UMBM sub-test called "Bi-Directional square path Test (BDT)”. In BDT the robot is programmed to follow a 4×4 m square path in clockwise (CW) and then counter-clockwise (CCW) directions. Upon completion of the square path in each direction, the experimenter again measures the absolute position of the vehicle. Then these absolute measurements are compared to the position and orientation of the vehicle as computed from odometry data [7]. The coordinates of the two centers of gravity are computed as follow:

$$X_{CW,CCW} = \frac{1}{n}\sum_{i=1}^{n} x_{CW,CCW} \quad (6)$$

$$Y_{CW,CCW} = \frac{1}{n}\sum_{i=1}^{n} y_{CW,CCW} \quad (7)$$

where n is the number of test trials in each direction and supposed to 10 in the following experiments.

A. Error Classification

The errors are categorized into type A and type B. Type A errors are caused mostly by E_b and cause too much or little turning at the corners of the square path. The amount of rotational error in each nominal 90 turn is denoted by α and β measured in radian. Type B errors are caused mostly by the ratio between wheel diameters E_d and they cause a slight curved path instead of a straight one during the four straight legs of the square path. Because of the curved motion, the robot will gain an incremental orientation error β, at the end of each straight leg (Fig. 9). α and β can be found from simple geometric relations.

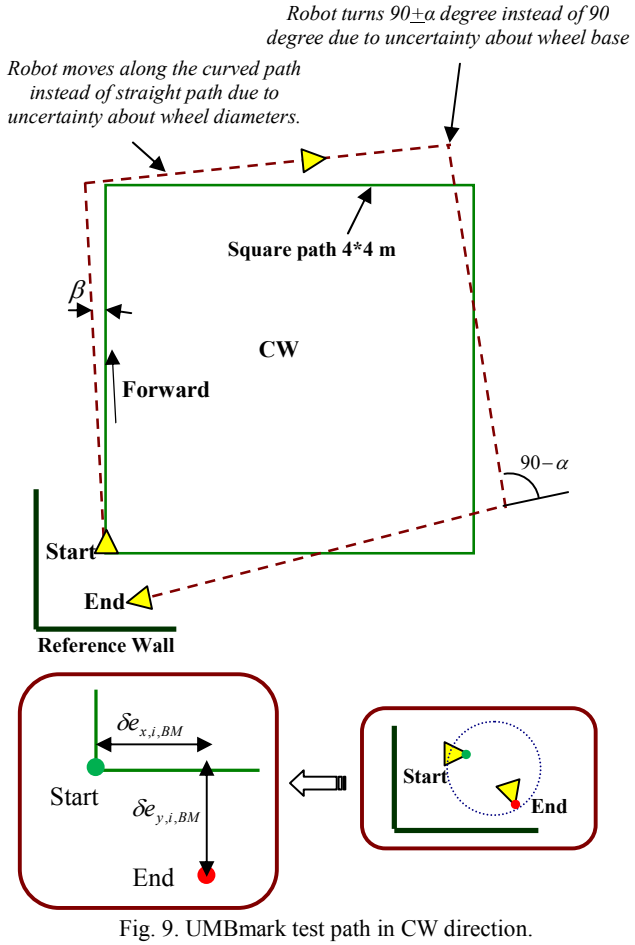

Fig. 9. UMBmark test path in CW direction.

$$\alpha = \frac{180}{n}.\frac{X_{CW}+X_{CCW}}{-4L} \quad (8)$$

$$\beta = \frac{180}{n}.\frac{Y_{CW}-Y_{CCW}}{-4L} \quad (9)$$

where L is straight leg of the square path and considered 4 m for this study.

Finally, two correction factors can be defined by [7]:

$$c_L = \frac{2}{E_d+1} \quad (10)$$

$$c_R = \frac{2}{\frac{1}{E_d}+1} \quad (11)$$

To compare the robot errors during the experiments and better presentation of robots position in each trial, the radial error of robot center (δe_r) is defined as follows:

$$\delta e_r = \sqrt{(\delta e_x)^2 + (\delta e_y)^2} \quad (12)$$

where δe_x and δe_y are depicted in Fig. 9.

Figure 10-a shows the schematic of experimental results in two CW and CCW directions, before and after calibration for vacuum cleaner robot. Also it demonstrates the contribution of two type errors (Types A and B) labeled with α and β angles. The coordinates of stop points, which are the radial error, are plotted in Fig. 10-b. These figures show a clear pictorial understanding of systematic errors improvement. The data shown in Figs. 10-a and 10-b confirm that the errors of robot in motion were reduced after applying the related coefficients.

Fiugure 11 illustrates the radial positioning error of robot in both CW and CCW directions. As depicted, in each trial, the radial errors was reduced after calibration which shows the effectiveness of the calibration method. Based on the UMBmark test results, the mean error improvement index was obtained equal to 83.0% and 84.4% for CW and CCW tests, respectively, which shows the effectiveness of calibration process. The similar results are shown in Fig. 12 for searching robot, R2.

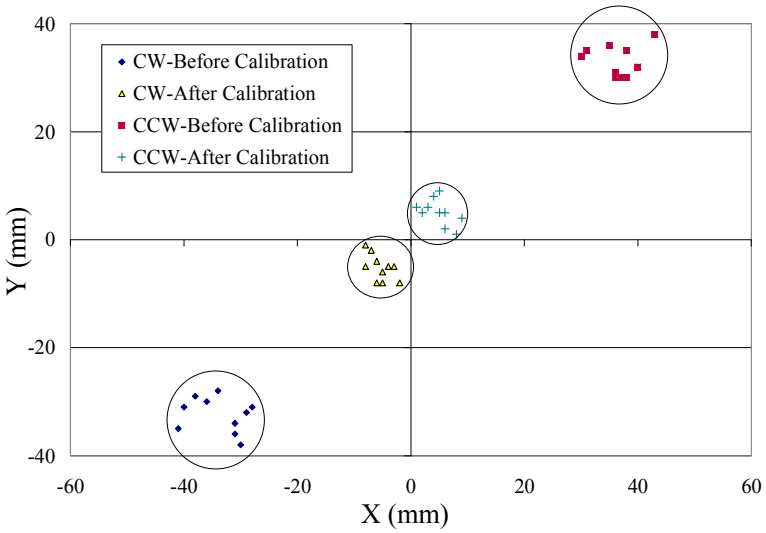

(a)

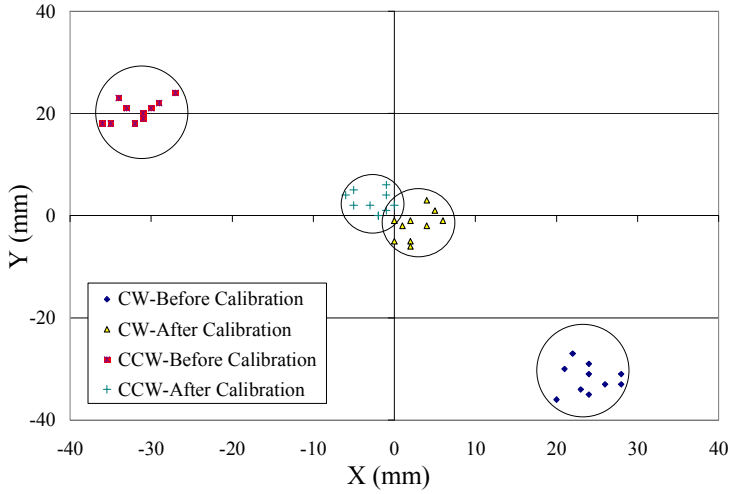

(b)

Fig. 11. Experimental results of UMBmark test.

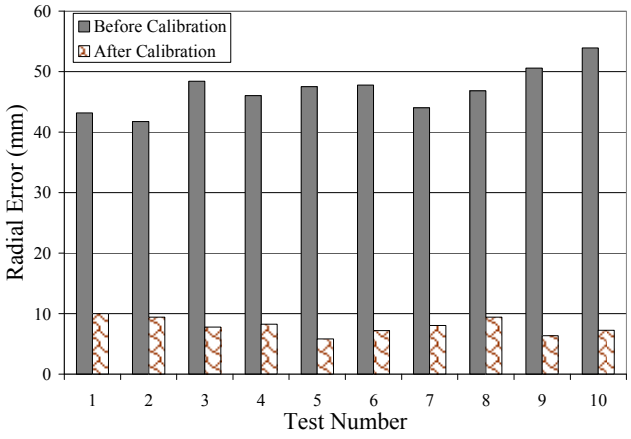

CW direction

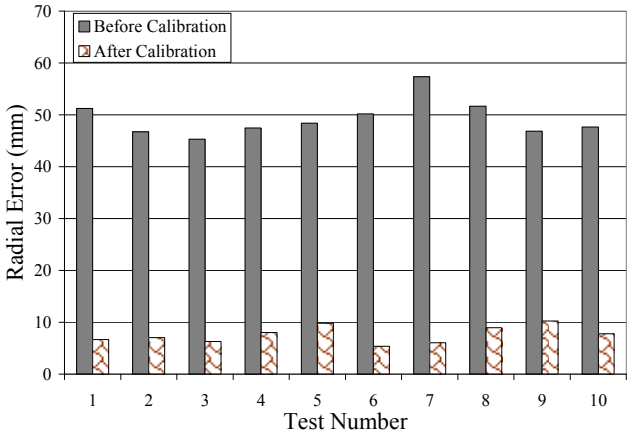

CCW direction

Fig. 11. Radial error in both CW and CCW directions, before and after calibration for R1.

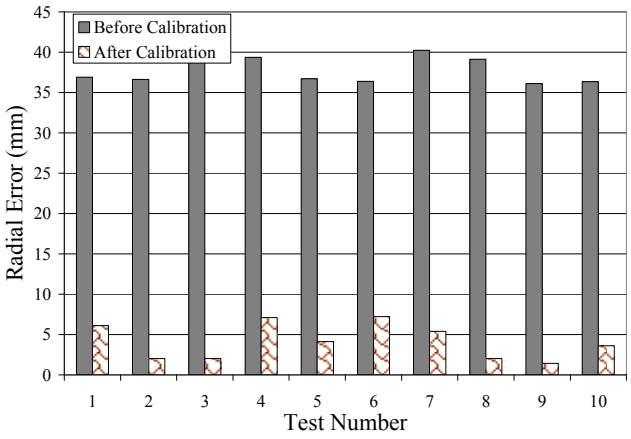

CW direction

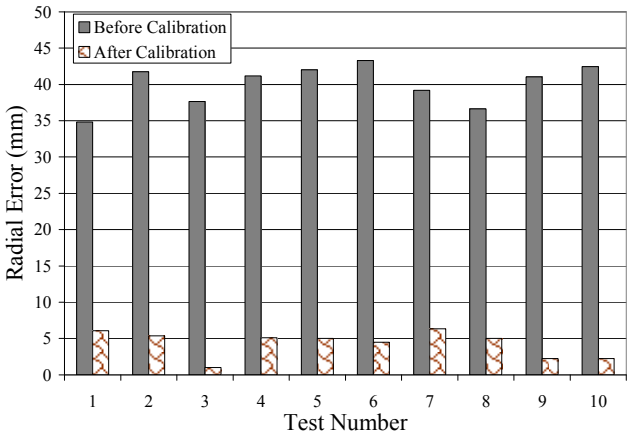

CCW direction

Fig. 12. Radial error in both CW and CCW directions, before and after calibration for searching robot.

V. Conclusions

This article addressed the design process and experimental results of two different types of mobile robots with differential drive mechanism which are manufactured as service robots. The design process started by defining the required robots parameters for either the house cleaning or searching purpose. To start the design process, first the kinematics and dynamics equations of differential drive robots were derived in a symbolic form assuming that no slip occurred on the wheels in the self-revolute rotation. It was followed by the simulation results performed using the student version of Adams software to calculate the characteristics of actuators and robot body. The design characteristics and control system implemented were then presented. Finally, some experiments were performed on the both prototype robots and positioning errors of robots were reduced using commonly used approach called the University of Michigan Benchmark (UMBmark) method. Furthermore, the radial error index was statistically defined to measure the workability of benchmark test. The experimental study indicated the positioning error improvement above 83% for both robots.

References

[1] Wuensch, K. L., "*Encyclopaedia of Statistics in Behavioural Science*," Wiley, United Kingdom, 2005.

[2] Y. Maddahi and A. Maddahi, "Mobile Robots Experimental Analysis Based on Kinematics," WSEAS *Transactions on Circuits and Systems*, vol. 3, 2004, pp. 1662-1667.

[3] K. Jung-Hwan, H. Dong-Choon, J. Yong-Woo and K. Eun-Soo, "Intelligent Mobile Robot System for Path Planning Using Stereo Camera-Based Geometry Information," *Proceeding SPIE - International Soc. Opt. Eng.,* vol. 6006, 2005, pp. 60060L-1-12.

[4] M. Piaggio, A. Sgorbissa and R. Zaccaria, "Navigation and Localization for Service Mobile Robots Based on Active Beacons," *Journal of Systems Science* 27, Issue 4, 2001, pp. 71-83.

[5] B. Bury and J. C. Hope, "Autonomous Mobile Robot Navigation Using a Low-cost Fibre Optic Gyroscope," *International Conference on Intelligent Autonomous Vehicles*, Finland, 1995, pp. 39-43.

[6] W. Kwon, K. S. Roh and H. K. Sung, "Particle Filter-Based Heading Estimation Using Magnetic Compasses for Mobile Robot Navigation," *International Conference on Robotics and Automation*, USA, 2006, pp. 2705-12.

[7] Borenstein J. and Feng L., " Correction of Systematic Odometry Errors in Mobile Robots, "*International conference on Intelligent Robots and systems*, 1995, pp.569-574.

[8] Borenstein. J, Everett. H. R. and Feng. L., "Mobile Robot Positioning: Sensors and Techniques", Journal of Robot. Syst., vol. 14, 1997, pp. 231–249.

[9] Maddahi Y., Sepehri N., Ghorabi H. and Maddahi A., "Testing Robotic Manipulator: Improvement and Experience", *International Journal of Systems Applications, Engineering and Development*, 2010, pp. 35-45.

[10] Maddahi Y., Hosseini Monsef S. M. and Maddahi A., "Experimental Tests of Wheeled Mobile Robots Using Mathematical Formulations", *Journal of Science and Technology*, vol. 1, 2008, pp. 3-8.

[11] Y. Maddahi and A. Maddahi, "YMBM: New Method for Errors Measurement in Wheleed Mobile Robots", *WSEAS Transactions on Systems*, vol. 5, 2006, pp. 552-557.

[12] M. Abdolmohammadi, A. Maddahi and Y. Maddahi, "Comparative Study of Two-wheeled Mobile Robots Performance", *International Conference on Manufacturing Engineering*, Iran, 2010.

[13] Denavit J., Hartenberg R. S., "A Kinematic Notation for Lower-Pair Mechanisms Based on Matrices", *ASME Journal of Applied Mechanics*, 1955, pp. 215-221.

[14] S. M. Hosseini Monsef, Y. Maddahi and A. Maddahi, "Service Robots: Design and Construction" International Conference on Applied Mathematics, Simulation, Modelling, Greece, pp. 45-50, 2011.

[15] Y. Maddahi, M. Seddigh, M. Mohammad Pour and M. Maleki, "Simulation Study and Laboratory Results of Two-wheeled Mobile Robot," *WSEAS Transactions on Systems*, vol. 3, 2004, 2807-2812.

Y. Maddahi received his M.Sc. degree in Mechanical Engineering from the Iran University of Science and Technology, Tehran, Iran, in 2003. Currently he is pursuing his Ph.D. degree in the Mechanical and Manufacturing Engineering at the University of Manitoba, Winnipeg, Manitoba, Canada. He became member of IEEE, ASME and CSME in 2009. He was faculty member in Mechanical Engineering department at Islamic Azad University (Saveh Branch). His research interests are in the area of test and calibration of mobile robots and manipulators, redundancy resolution techniques, manipulability of robotic systems, and performance analysis of mobile manipulators.

S. M. Hosseini Monsef received the B.Sc. degree in Mechanical Engineering from Ferdowsi University of Mashhad and M.Sc. from Islamic Azad University, Iran. He is currently faculty member at the Mechanical Engineering department at the Islamic Azad University (Saveh Branch). His current research interests include application of mechatronic systems in engineering and nonlinear vibration.

A. Maddahi received his B.Sc. degree in Mechanical Engineering from Amir Kabir University of Technology (Tehran Polytechnic) and now is the graduate student in Mechanical Engineering at K. N. Toosi University of Technology, Tehran, Iran. His current research is in the area of control of robotic systems, test and calibration of mobile robots and improvement of industrial robotic manipulators.

R. Kalvandi is the BSc. student in Science at the University of Winnipeg, Winnipeg, Canada. Her current research is in the area of risk assessment and hazardous analysis of service/assistant machines especially those which are used in the medical environments and standards of medical instruments and devices.